Modeling and Experimental Investigation of Grid-Connected PWM Rectifier

K. Fahem*, D. Chariag* and L. Sbita*

ABSTRACT

Due to the huge amount of polluting loads connected to the grid, the power quality of the grid has become an interesting concern. The grid-connected PWM Rectifiers are widely employed in this case because they provide low harmonic distortion as well as high power factor. Conventionally these converters are controlled using the decoupled d-q vector control based on PI regulators. However the practical study of this paper shows poor performance of the control system under unbalanced grid.In this paper a mathematical model ofthe grid-connected PWM rectifieralso known as the voltage source PWM converter (VSC) is presented. The implemented control strategy has been presented in details and simulated in MATLAB/ SIMULINK environment and an experimental setup has been builtbased on dsPACE system with DS1104 controller board and SEMIKON inverter. Then two switching pattern, the sinusoidal pulse width modulation (PWM) and the space vector modulation (SVM), are implemented to compare their performance under unbalanced power grid in term of total harmonic distortion (THD).

Keywords: PWM rectifier; VOC;PI tuning; SVM; total harmonic distortion.

1. INTRODUCTION

As a first stage of power conversion, grid-connected PWM rectifier has been widely used in power systems such as uninterruptible power supplies [1], adjustable-speed drives [2], battery energy storage systems [3] and recently becomes an interesting research subject in renewable power generation systems [4]. By providing low harmonic distortion and high power factor, PWM rectifier presents a perfect solution for harmonic problems produced by traditional power electronics devices (diodes and thyristors bridge converters) also it ensures a bidirectional power flow between the power supply and the active load [5-6].

Although PWM rectifier has been well used in many industrial applications, it is still difficult to control it due to its multi-input multi-output nonlinear structure hence many control strategies have been presented in the literature, the most conventional one is the voltage oriented control (VOC) using PI controllers. It attempts to achieve an accurate output voltage level using an outer voltage loop and fulfill high power factor condition using two inner current loops. On the other hand, the selection of the switching technique is a critical aspect in the design of the control system especially in term of low harmonic distortion. The sinusoidal pulse width modulation (SPWM) is well used in power electronics control but it is weakly useful in reducing harmonic current distortion compared with the space vector modulation which provides better harmonic distortion reduction [7]. Adaptive hysteresis band current control (HBCC) has a better dynamic performance but it is a variable switching frequency technique which could bring increased switching losses [8].Some recent control methods are discussed in [21-25].

This paper is organized as follow: in section 1, a mathematical model of three–phase voltage source PWM converter is presented both in the three-phase coordinates and the two-phase stationary coordinates, then a study of the decoupled d-q vectorcontrol strategy is carried on as well as the selection of the PI

---
*   Research Unitof Photovoltaic, geothermal and Eolian Systems National School of Engineers of Gabes, University of GabesSt Omar Ibn El-Khattab, 6029 Gabes, Tunisia, *Emails: kawther.fahem@hotmail.fr, dhia.chariag@gmail.com, lassaad.sbita@gmail.com*

regulators for each control loop. Simulation model is built in MATLAB/SIMULINK environment to verify mathematical model and the chosen control method and DSP- based control system has been built in the laboratory to validate theoretical results in section 2. Then a comparison study between sinusoidal pulse width modulation (PWM) and space vector modulation (SVM) techniques under unbalanced grid will be carried out in section 3 in order to reduce harmonic current distortion.

2. MATHEMATICAL MODEL AND CONTROL STRATEGY OF THE VSC

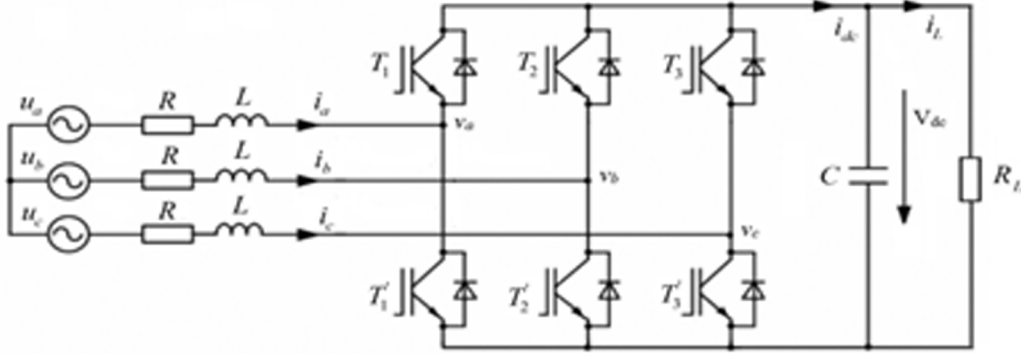The three phase voltage source PWM rectifier circuit diagram is shown in Figure 1.

Figure1: PWM rectifier circuit diagram

We assume that the three phase system is balanced (1) and the IGBT is ideal.

Also, u_a, u_b and u_c present the phase voltages and i_a, i_b and i_c are the phase currents, R and L are the resistance and the inductance of the line reactor respectively, i_{dc} and i_L are the DC output current and the load current respectively and C is the dc-link capacitor.

$$\begin{cases} u_a + u_b + u_c = 0 \\ i_a + i_b + i_c = 0 \end{cases} \tag{1}$$

The mathematical model of three-phase PWM rectifier in the three-phase stationary coordinates is presented in (2) and (3)

$$\begin{bmatrix} u_a \\ u_b \\ u_c \end{bmatrix} = L\frac{d}{dt}\begin{bmatrix} i_a \\ i_b \\ i_c \end{bmatrix} + R\begin{bmatrix} i_a \\ i_b \\ i_c \end{bmatrix} + V_{dc}\begin{bmatrix} S_a \\ S_b \\ S_c \end{bmatrix} \tag{2}$$

$$C\frac{dV_{dc}}{dt} = \sum_{k=a}^{c} i_k S_k - i_L \tag{3}$$

By applying the Park transformation in the d-q rotating coordinate to (2) and (3), the mathematical model of the VSC becomes;

$$\begin{bmatrix} u_d \\ u_q \end{bmatrix} = L\frac{d}{dt}\begin{bmatrix} i_d \\ i_q \end{bmatrix} + \begin{bmatrix} R & -wL \\ R & wL \end{bmatrix}\begin{bmatrix} i_d \\ i_q \end{bmatrix} + V_{dc}\begin{bmatrix} S_d \\ S_q \end{bmatrix} \tag{4}$$

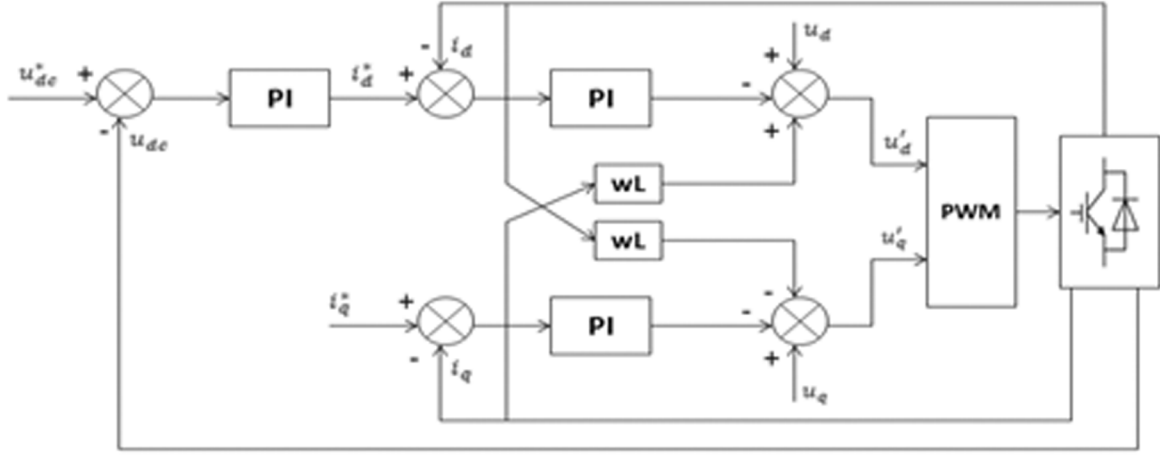$$C\frac{dV_{dc}}{dt} = \frac{3}{2}(i_d S_d + i_q S_q) - i_L \tag{5}$$

Figure2: The decoupling feed-forward control loop block diagram

Voltage oriented control strategy is composed basically of an outer voltage loop which attempts to maintain an accurate dc-link voltage level followed by two inner current loops to achieve unity power factor condition.

Looking at the mathematical model of the VSC, it is clear that there is a mutual coupling between the two currents i_q and i_d with (wLi_d) and (wLi_q) terms. So by using a decoupled feed-forward control strategy they canbe controlled independently and this also reduces the current loop to a first order plant and improves the tracking performance [9].

2.1. The inner current loop

The inner current control loop contains two PI controllers; basically they tend to regulate the active and reactive current i_d and i_q respectively. The d-axis current loop attempts to maintain a constant DC voltage by tracing the reference current value i_d^* produced by the outer voltage loop. In order to fulfill the unity power factor condition, the q-axis current component i_q^* has to be set to zero [10].

Transforming (4) into (6):

$$V_{dc}\begin{bmatrix} S_d \\ S_q \end{bmatrix} = \begin{bmatrix} u_d \\ u_q \end{bmatrix} - L\frac{d}{dt}\begin{bmatrix} i_d \\ i_q \end{bmatrix} - \begin{bmatrix} R & -wL \\ R & wL \end{bmatrix}\begin{bmatrix} i_d \\ i_q \end{bmatrix} \tag{6}$$

Then, the d-q voltage commands are expressed as follow, where $u_d' = S_d V_{dc}$ and $u_q' = S_q V_{dc}$:

$$\begin{cases} u_d' = u_d + wLi_q - \left(Ri_d + L\dfrac{di_d}{dt} \right) \\ u_q' = u_q - wLi_d - \left(Ri_q + L\dfrac{di_q}{dt} \right) \end{cases} \tag{7}$$

The d-q voltage commands can be controlled as follow:

$$\begin{cases} u_d' = -\left(K_{ip} + \dfrac{K_{il}}{s} \right)\left(i_d^* - i_d \right) + wLi_q + u_d \\ u_q' = -\left(K_{ip} + \dfrac{K_{il}}{s} \right)\left(i_q^* - i_q \right) - wLi_d + u_q \end{cases} \tag{8}$$

Assuming that open loop of transfer function of the current controller can be expressed as follow:

$$H_c(s) = \frac{K_{ip}(1+sT_i)}{sT_i} \frac{1}{1+sT_s} \frac{K_{pwm}}{1+T_{pwm}} \frac{1}{R+sL} \tag{9}$$

Where K_{ip} and T_i are the gain and the time constant of PI regulator respectively, the sample block can be presented as a first order lag with time constant T_s andthe PWM block is approximatedalso to a first order lag with gain K_{pwm} and time constant T_{pwm}.

The sampling and the PWM block introduced to the system a digital delay with small value $T_s + T_{pwm} = 1.5T_s$.
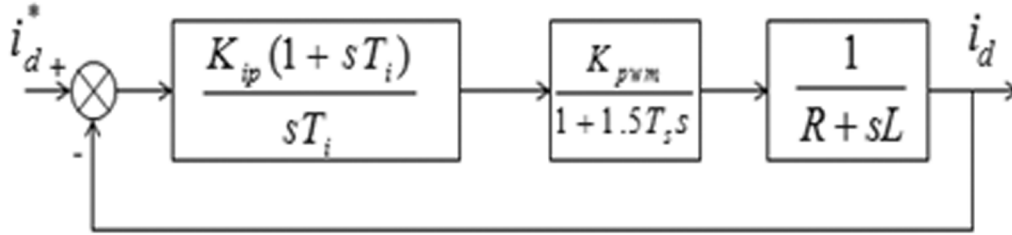

Figure 3: The d-axis current control loop diagram

Then the inner current control loop of the d-axis current is presented:

The open loop transfer function of the previous system is expressed as follow:

$$H_o(s) = \frac{K_{ip}(1+sT_i)K_{pwm}}{sRT_i(1+1.5sT_s)} \tag{10}$$

To simplify the previous transfer function, the integral time constant of the PI regulator should be selected equal to the time constant of the load. Then the closet loop transfer function presented as:

$$H_c(s) = \frac{K_{ip}K_{pwm}}{1.5RT_iT_ss^2 + RT_is + K_{ip}K_{pwm}} \tag{11}$$

The PI regulator can be tuned using the conventional pole placement criteria, choosing the damping factor equal to D = 0.707 to get an optimum phase margin , the proportional and the integral gains of the PI regulator are determined by (12). Figure 5.a shows the bode plot of open loop transfer function with these determinate parameters; the crossover frequency is about 482 Hz,given a phase margin of 66°.

$$\begin{cases} K_{ip} = \dfrac{RT_i}{3T_sk_{pwm}} \\ K_{iI} = \dfrac{K_{ip}}{T_i} \end{cases} \tag{12}$$

2.2. The outer voltage loop

The dc-link dynamic model was given in (3), considering the power balance equation between the ac source and the dc load (13), the reactive voltage component of the ac source was eliminated ($u_q = 0$), it is

observed in (14) that the dc-link voltage equation is non-linear. So simplification of such equation is employed by the linearization of the model around an operating point as well as considering i_L as a disturbance and i_d the only input of the system.

$$\frac{3}{2}(u_d i_d + u_q i_q) = V_{dc} i_{dc} \tag{13}$$

$$\frac{dV_{dc}}{dt} = \frac{3}{2}\frac{u_d}{CV_{dc}}i_d - \frac{i_L}{C} \tag{14}$$

Using small signal approximation, the dc-link model in Laplace domain becomes:

$$\frac{V_{dc}(s)}{i_d(s)} = \frac{3}{2}\frac{u_d}{V_{dc,ref}}\frac{1}{sC} \tag{15}$$

The sample and hold block are presented by first order transfer function with time constant $T_c = T_s$ and the closed-loop transfer function of the inner current regulator has been approximated to a first order transfer function with time constant $T_q = 2*1.5T_s$ [10]. So the open loop transfer function of the outer voltage loop can be expressed:

$$H_{vo}(s) = \frac{K_{up}(1+sT_u)}{sT_u}\frac{1}{1+sT_c}\frac{1}{1+sT_q}\frac{1}{sC} \tag{16}$$
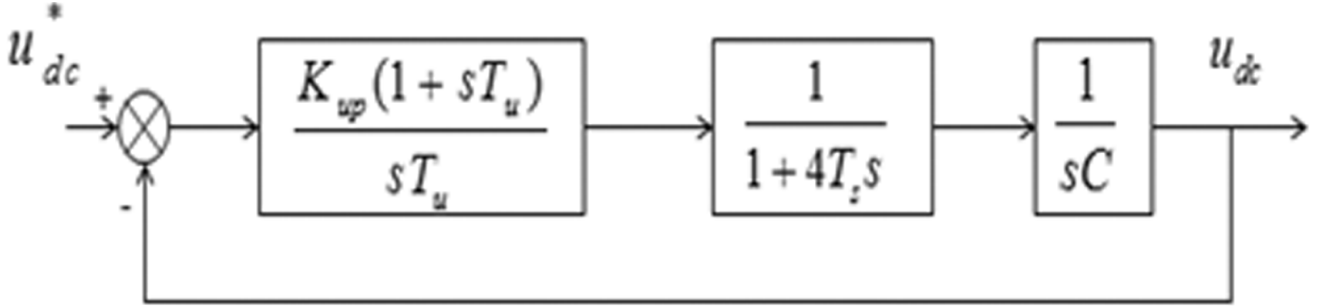

Figure 4: The DC-voltage loop control diagram

The outer voltage loop regulator is given in Figure 4.

Then open-loop transfer function of this voltage control loop becomes:

$$H_v(s) = \frac{K_{up}(1+sT_u)}{sT_u(1+4T_s s)sC} \tag{17}$$

According to [10-14], it is noted that for such open loop transfer function which included a dominant time constant (T_u) and a minor time constant (T_s) the symmetrical optimum (SO) method is used for adjusting the PI regulator.

The system bandwidth has been proposed in [14]. Choosing the value of 'a' is very critical for the selection of the PI parameters because low values of the chosen bandwidth could influence the system stability whereas higher values led to slow dynamic response. Figure 5.b shows the bode plot of open loop transfer function with these determinate parameters; the crossover frequency is about 42 Hz, given a phase margin of 45°.
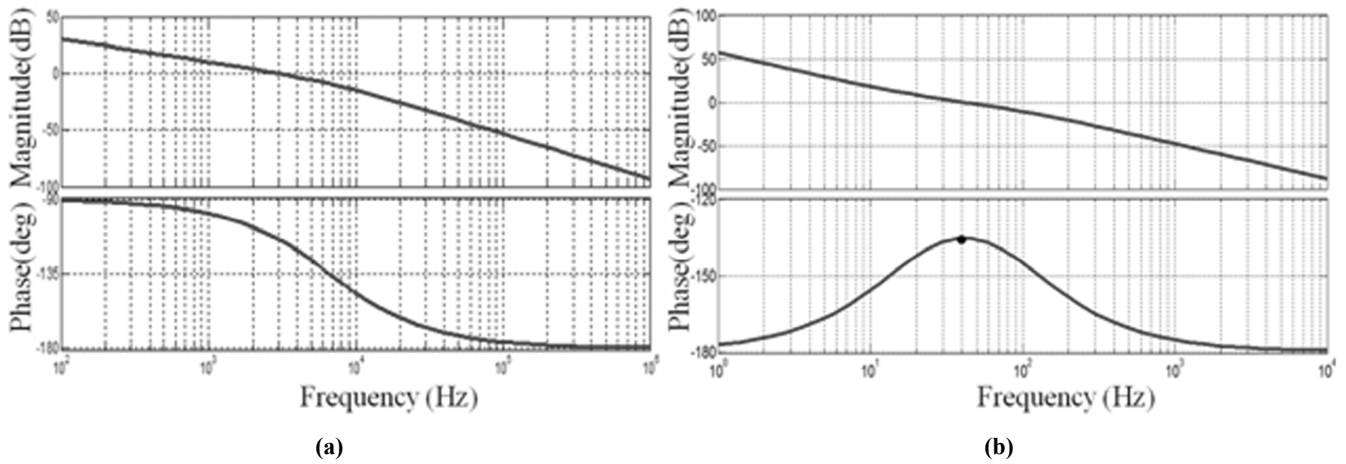
(a)

(b)

Figure 5: Bode diagram (a) current loop control (b) voltage loop control

3. SIMULATION AND EXPERIMENTAL RESULTS

A simulation model of the grid-connected PWM rectifier was built in MATLAB/SIMULINK environment. The mathematical model and the control strategy studied above were implemented on the simulation.

The parameters of the inner current loop and the outer voltage loop are: K_{ip} =1 .69, K_{ii} = 260, K_{up} = 29.04, K_{ui} = 12600. Then a laboratory setup was built using dsPACE system with DS1104 controller board and SEMIKON inverter. The system parameters shown in Table 1 are the same for both the simulation model and the experimental setup.

(a)

(b)

(c)

(d)

(e)   (f)
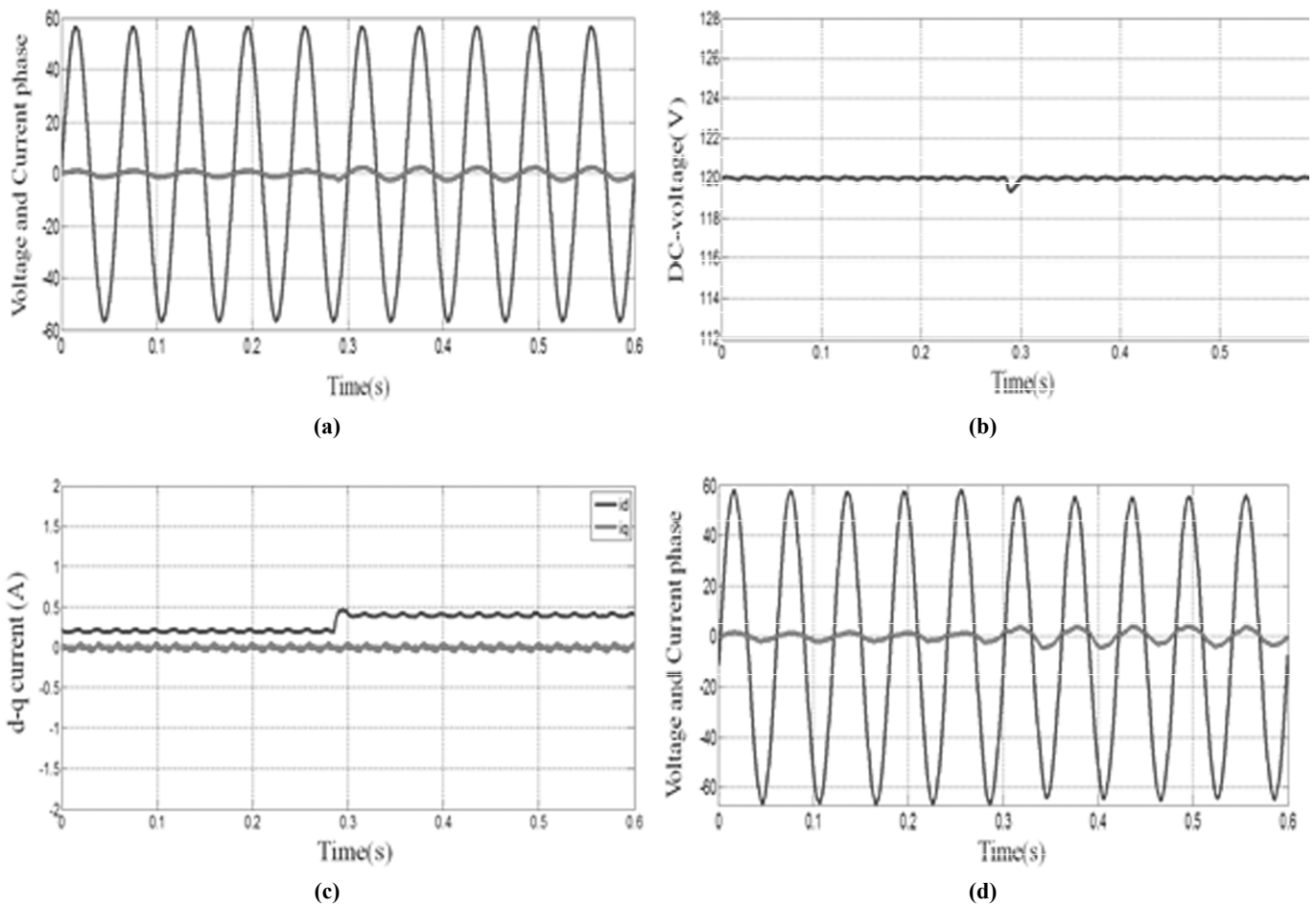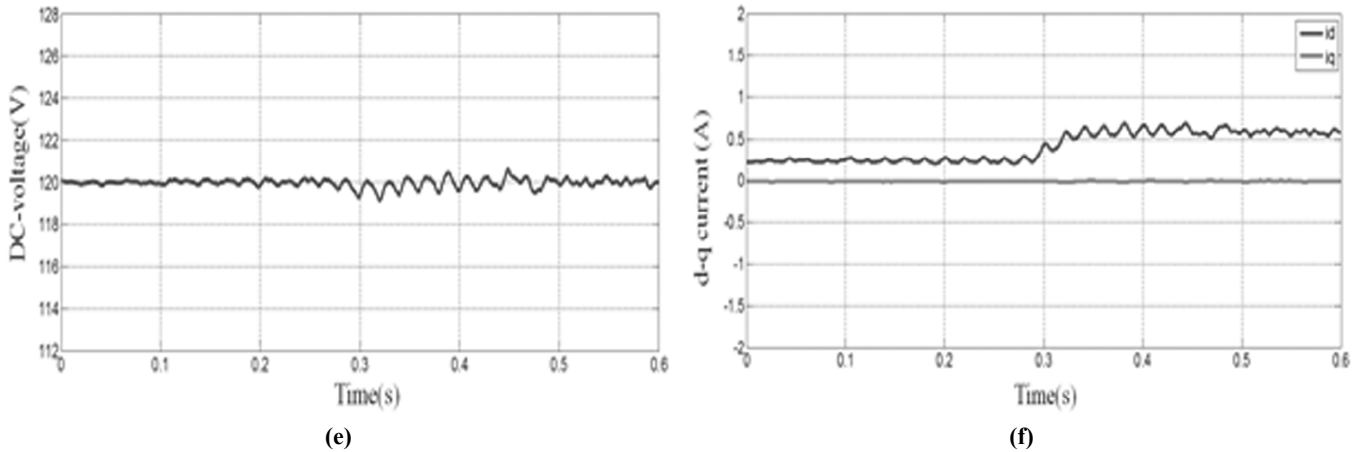
Figure 6: Simulation results (a) voltage and current phase (b) DC-link voltage (c) d-q current and experimental results (d) voltage and current phase (e) DC-link voltage (f) d-q current
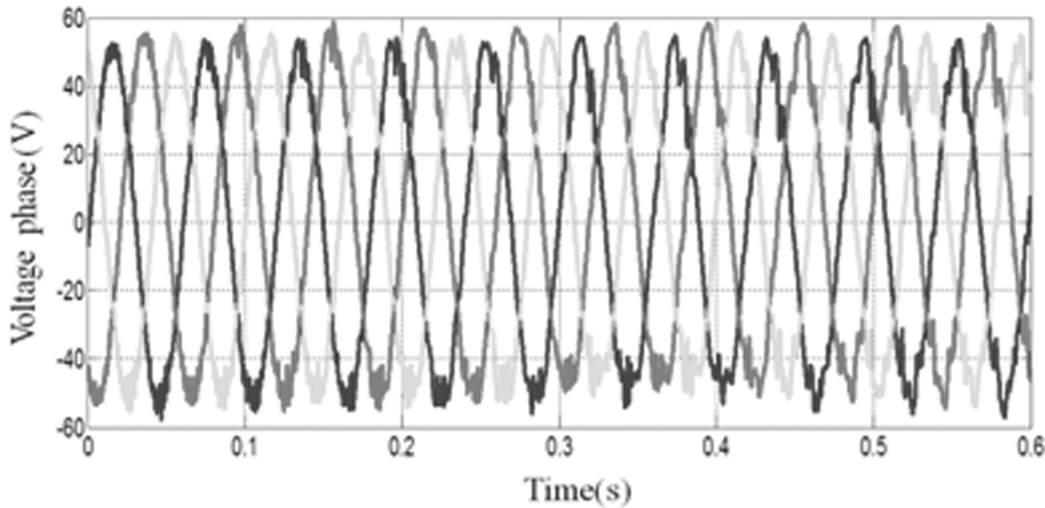

Figure 7: Three-phase unbalanced voltage grid

The simulation results demonstrate that grid-connected PWM rectifier can assure an accurate DC-link voltage, provide a sinusoidal AC current waveform and achieve unit power factor ($i_q = 0$) as it is shown in Figure 6. Figure 6.a shows that the current waveform is perfectly sinusoidal and has the same phase as the voltage waveforms.It is clearly shown in Figure 6.b that the system has a good dynamic response to the variation load. The reactive current continued zero even with load variation as it is shown in Figure 6.c.

Looking at the experimental results, we can see in Figure 6.d that the current waveform is not perfectly sinusoidal which indicates the presence of unwanted harmonic pollution. Also in Figure 6.e and figure 6.f show the existent of oscillations in active and reactive currents and the dc-link voltage is increasingly distorted, these defects can be explained by the current distortion caused by the nonlinear load and on the other hand by the distortion of the grid voltage and the unbalanced voltage level of the grid phases as it is shown in Figure 7, also the interaction between both current and voltage loop control could bring voltage distortion in the dc-link output and influence the current loop dynamic [15-16]. It must be noted that a low-pass filter has been added to the experimental results which cover the effect of anti-aliasing filter.

In order to confirm the effects of the unbalanced grid on the system performance, it had been taken into account in the simulation lab. Figure 8 indicates that both the simulation and experimental results show the same poor performance under unbalanced grid.
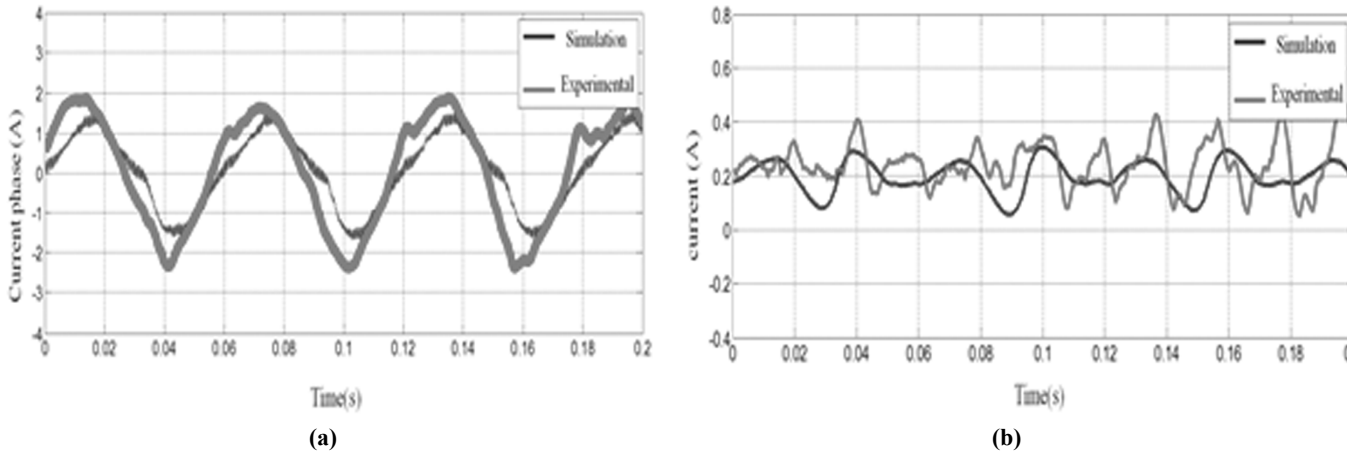
(a)   (b)

Figure 8: Simulation and experimental results under unbalanced grid
(a) grid current phase waveforms (b) active current i$_d$ waveforms

4.   COMPARISON STUDY BETWEEN PWM AND SVM

The aim of this study is to select the appropriate switching technique that provides a better current harmonic reduction under disturbed voltage grid. Although SVM has become widely used in power converters due to its optimum switching patterns, it is more complex and difficult to implement than the conventional PWM technique [17-19].The comparison has been carried out in MATLAB/SIMULINK environment. The
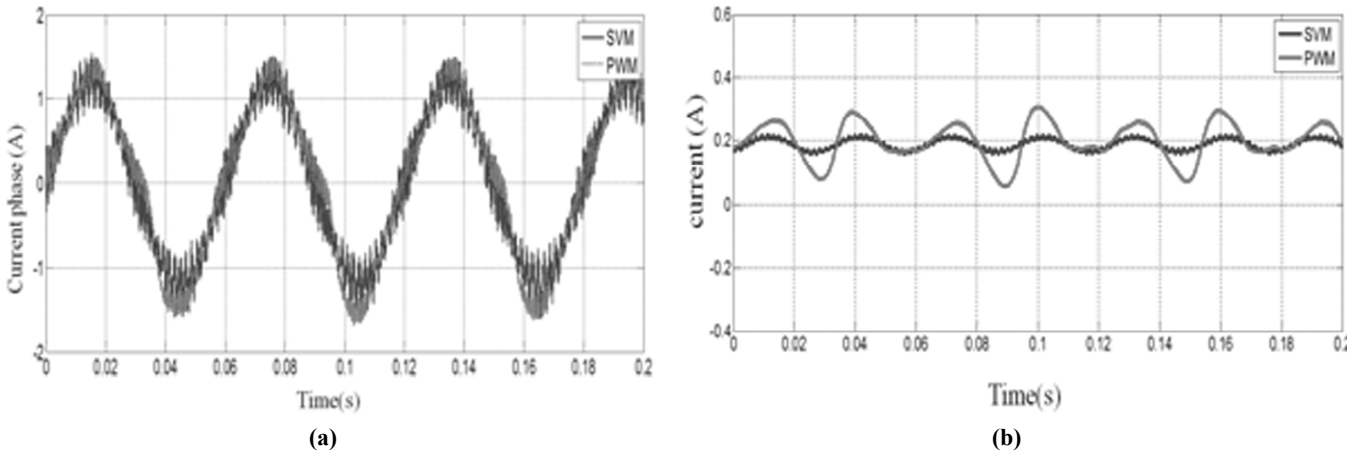

(a)   (b)

Figure 9: Simulation results under unbalanced grid of PWM and SVM techniques
(a) grid current phase waveforms (b) active current i$_d$ waveforms

(a)   (b)
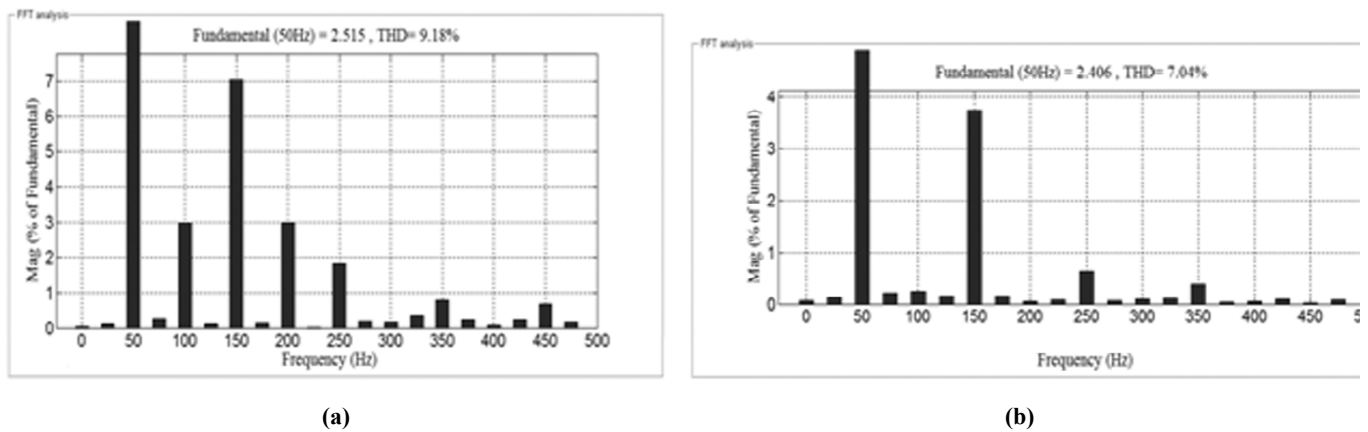
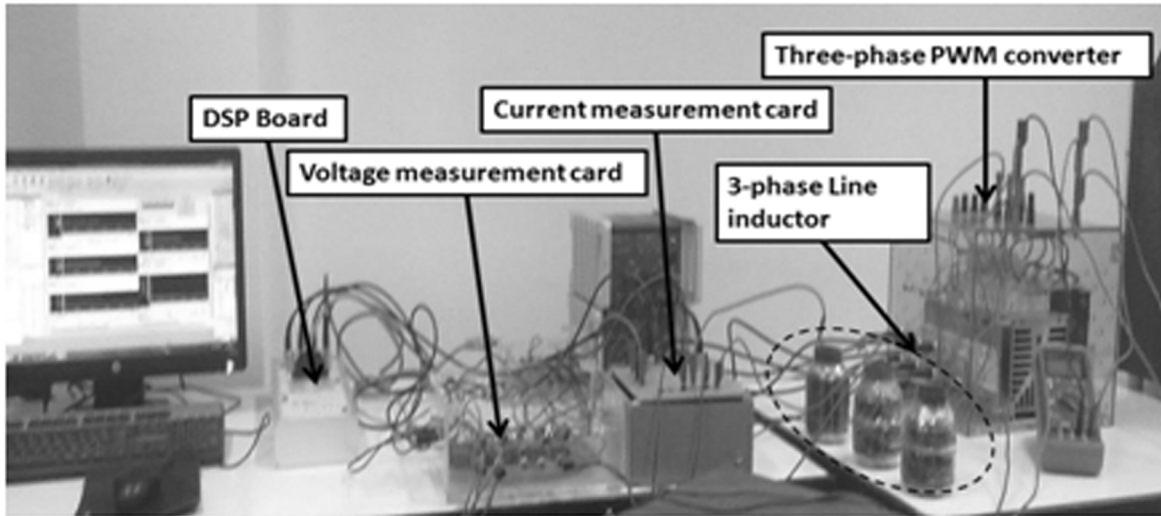**Figure 10: THD analysis for (a) PWM and (b) SVM techniques**

Figure 11: Laboratory setup of the three-phase PWM rectifier

simulation results are presented in figure9 and 10, it shows that SVM ensures better sinusoidal current waveform than PWM technique and it has less total harmonic distortion under unbalanced grid voltage.

5. CONCLUSION

In this paper, a grid-connected PWM rectifier model has been analyzed and simulated. The mathematical model and the decoupled feed-forward control strategy are both validated by the result of the simulation in the MATLAB/SIMULINK environment and the experimental setup. Simulation results show that the system has high power factor, good dynamic response and accurate DC-link voltage level. But in practical test the conventional control scheme shows poor performance in harmonic distortion rejection and weak reduction of the system noise under steady state conditions of the dc-link voltage controller. So in order to ameliorate the control system performance under unbalanced voltage grid another switching technique has been implemented in the simulation lab, SVM switching technique shows better current harmonic distortion reduction than PWM switching technique which makes it more suitable for grid-connected rectifier application. In future work implementation of the selected switching technique in practical lab should be carried out to confirm theoretical results also the bandwidth of the dc-link voltage controller should be selected much lower than the grid frequencyand an extended study of the system nonlinearity model must be taking into account rather than linearization of the model around a specific operation point which is not always valid [20].

APPRENDIX

Table 1
System parameters

Parameter	Symbol		Value
Nominal power		P	500 W
Grid phase voltage		V_b	56.5 V
Grid frequency		f	50 Hz
DC-link voltage		V_{dc}	120 V
DC-link capacitance		C	1100 μF
Filter resistance		R	0.75 Ω
Filter inductance		L	5 mH
Switching frequency	f_s	10 kHz	

REFERENCES

[1]   H. Lei, E. Xiao, J. Xiong, X. Linand Y. Kang, "Modeling and analysis of three-phase four-leg PWM boost-type rectifier for double conversion transformerless UPS," Proceedings of the 37th AnnualConference on IEEE Industrial Electronics Society (IECON-2011), 1444 – 1449, 2011.

[2]   M.H. Hedayati, A.B. Acharya and V. John, "Common-mode filter design for PWM rectifier-based motor drives," *IEEE Transactions on Power Electronics*, **28** (11), 5364–5371, 2013.

[3]   M.P. Akter, S. Mekhilef, N.M.L. Tan and H. Akagi, "Model predictive ontrol of bidirectional AC-DC converter for energy storage system," *Journal of Electrical Engineering & Technology*, **10** (1), 165-175, 2015.

[4]   R. Teoderescu, M. Liserre and P. Rodriguez, *Grid Converters for Photovoltaic and Wind Power Systems*, John Wiley, London, 2011.

[5]   B. Singh, B.N.Singh, A. Chandra, K. Al-Haddad, A. Pandey and D. P.Kothari, "A review of three-phase improved power quality AC-DC converters", *IEEE Transactions on Industrial Electronics*, **51** (3), 2004.

[6]   J.A.A. Caseiro and A.M.S. Mends, "Performance analysis of three-phase PWM rectifiers for high power quality applications", Proceedings of the International Conference on Renewable Energies and Power Quality (ICREPQ-2009), Valencia, 2009.

[7]   N. S. Ting, Y. Yasa , I. Aksoy and Y. Sahin, "Comparison of SVPWM, SPWM and HCC control techniques in power control of PMSG used in wind turbine systems," Proceedings of the IEEE International Aegean Conference on Electrical Machines & Power Electronics (ACEMP-2015), Side, Turkey, 69-74, 2015.

[8]   S. Jena, B.Chitti Babu, S.R.Samantaray and M. Mohapatra, "Comparative study between adaptive hysteresis and SVPWM current control for grid-connected inverter", Proceedings of the 2011 IEEE Students' Technology Symposium (Tech-SIM),Jan. 14-16, Kharagpur, India, 310-315, 2011.

[9]   M. Malinowski, M. P. Kazmierkowski and A. Trzynadlowski, "Review and comparative study of control techniques for three-phase PWM rectifiers", *Mathematics and Computers in Simulation*, **63** (3-5), 349-361, 2003.

[10] V. Blasko and V. Kaura, "A new mathematical model and control of a three-phase AC-DC voltage source converter", *IEEE Transactions on Power Electronics*, **12** (1), 116-123, 1997.

[11] H. Wang and H. Qi, "Study of control strategies for voltage-source PWM rectifier", Proc. of the 2nd International Conference on Computer Science and Electronics Engineering (ICCSEE-2013), 1268-1271, 2013

[12] Y. Gao, J. Li and H.Liang, "The simulation of three-phase voltage source PWM rectifier,"Proceedings of the Asia-Pacific Power and Energy Engineering Conference (APPEEC-2012), Shanghai, March 27-29, pp. 1-4, 2012.

[13] X. Wang, H. Kaizheng, Y. Shijie and X. Bin, "Simulation of three-phase voltage source PWM rectifier based on direct current control", Proceedings of the Congress on Image and Signal Processing (CISP-2008), Sanya, China, May 27-30, pp. 194-198, 2008.

[14] C. Bajracharya, M. Molinas, J. A. Suul, T. Undeland, "Understanding of tuning techniques of converter controllers for VSC-HVDC," Proceedings of the Nordic Workshop on Power and Industrial Electronics, June 9-11, 2008.

[15] J. Miret, M.Castilla, J.Matas, J.M.Guerrero and J.C.Vasquez,"Selective harmonic-compensation control for single-phase active power filter with high harmonic rejection," *IEEE Transactions on Industrial Electronics*, **56** (8), 3117-3127, 2009.

[16] M. Zarif and M. Monfared, "Step-by-step design and tuning of VOC control loops for grid connected rectifiers," *International Journal of Electrical Power and Energy Systems*, **64**, 708-713, 2015.

[17] A. Hernandez, R.Tapia, O. Aguilarand A. Garcia, "Comparison of SVPWM and SPWM techniques for back to back converters in PSCAD," Proceedings of the World Congress on Engineering and Computer Science (WCECS-2013), Oct. 23-25, San Francisco, USA.

[18] A. Araújo, J. G. Pinto, B. Exposto, C. Couto and J.L. Afonso, "Implementation and comparison of different switching techniques for shunt active power filters," Proceedings of the 40th Annual Conference of the IEEE Industrial Electronics Society, Oct 29-Nov. 1, Dallas, TX, USA, pp. 1519-1525, 2014.

[19] J. Sabarad and G.H. Kulkarni, "Comparative analysis of SVPWM and SPWM techniques for multilevel inverter",Proceedings of the International Conference on Power and Advanced Control Engineering (ICPACE), Aug. 12-14, Bangalore, India, pp. 232-237, 2015.

[20] M.M. Amin and O.A. Mohammed, "DC-bus voltage control of three-phase PWM converters connected to wind powered induction generator," IEEE PES General Meeting, Minneapolis, MN, July 25-29, 2010.

[21] S. Sampath, S. Vaidyanathan and V.T. Pham, "A novel 4-D hyperchaotic system with three quadratic nonlinearities, its adaptive control and circuit simulation," *International Journal of Control Theory and Applications*, **9** (1), 339-356, 2016.

[22] S. Vaidyanathan and S. Sampath, "Anti-synchronization of identical chaotic systems via novel sliding control method with application to Vaidyanathan-Madhavan chaotic system", *International Journal of Control Theory and Applications*, **9** (1), 85-100, 2016.

[23] A. Sambas, S. Vaidyanathan, M. Mamat, W.S.M. Sanjaya, R.P. Prastio, "Design, analysis of the Genesio-Tesi chaotic system and its electronic experimental implementation", *International Journal of Control Theory and Applications*, **9** (1), 141-149, 2016.

[24] S. Vaidyanathan, K. Madhavan and B.A. Idowu, "Backstepping control design for the adaptive stabilization and synchronization of the Pandey jerk chaotic system with unknown parameters", *International Journal of Control Theory and Applications*, **9** (1), 299-319, 2016.

[25] A.T. Azar and S. Vaidyanathan, *Chaos Modeling and Control Systems Design*, Springer, Berlin, 2015.